BASELINE STABILIZATION ANALYSIS OF TETHERED InSAR SATELLITE SYSTEM DURING STATION KEEPING

Zhang Zhigang[(1)], **Zhang Jinxiu**[(2)], **Lan Shengchang**[(3)]
[(1)(2)] *Research Center of Satellite Technology, Harbin Institute of Technology,150080 Harbin,China, +86-451-86413440, zhdoug@gmail.com*
[(3)]*Department of Radio Science and Engineering, Aalto University, 02150, +358458567227, shengchang.lang@aalto.fi*

Abstract: *This paper mainly investigated the baseline variation during the station keeping of the InSAR tethered satellites system. A. Moccia made a study of the relationship between the wavelength and the baseline length. The effect of the dynamics of the system on the baseline needs to further research. A lumped massed model was used when researching the motion of the system during the station keeping. The dynamic equations could be derived through Newton-Eular laws. Then the baseline expression made up by the state parameters of the system was given. The results showed that the in-plan vibration and the out-plan vibration are the quasi-periodic motion and the amplitudes mainly determined by the initial parameters. The tether's shape was a curve whose curvature was changing along with time. The deviation between the mid of the instantaneous tether and the intermediate of the line from the mother-satellite to sub-satellite altered but the magnitude was pretty small. The tether flexibility has little effect on the baseline variation; however it is mainly determined by the in-plane vibration. From the numerical results, the conclusion that the satellites formation using space tether is a steady platform for the InSAR technology would be got.*

Keywords: *InSAR tethered satellites formation, station keeping, lumped massed model, baseline variation.*

1. Introduction

The concept of Tethered Satellite System (TSS) was put forward by Colombo et al. [1] in 1974, which evolved from the idea of Tsiolkovsky about the possibility of using a high tower from the equator to the geosynchronous altitude to escape the Earth's gravity [2]. Several missions were conducted in 1990s to verify the TSS concept and these missions proved the feasibility and survivability of TSS [3,4]. Meanwhile the dynamics and control of TSS were studied and a significant progress has been made [5,6,7]. The stability of the system was analyzed and different kinds of control methods were put forward during the different phases of the system [8,9,10]. Various applications of the TSS were put forward such as orbit transfer, formation flying, and artificial gravity and so on as the Ref [2] described.

The InSAR tethered satellites system was proposed by Antonio Moccia in 1986 [11]. He applied the tethered satellites technology into the height measurement with SAR

technology, which has a great progress and real product [12,13]. In his paper [14], he proved the tethered InSAR satellites system could be feasible in height measurement. Compared to the separated InSAR satellites system, it has an advantage on the fuel consumption for the reconfiguration of the formation could be seen as a unit when the system needs an orbital maneuver. The long and variable baseline make the InSAR tethered satellites system more promising as well. A. Moccia investigated the feasibility of the system and studied the relationship between the wavelength and baseline length. Therefore the effect of the dynamics of the system on the baseline need to further research. And the dynamics and control for tethered formation for space interferometry also were discussed in [15,16,17].

This paper mainly investigated the baseline variation during the station keeping of the InSAR tethered satellite system. When the dynamic equations of the system were derived, the lumped massed model was used. The shape of the tether was analyzed during this phase with different initial parameters. Then the baseline was expressed with the parameters of the system to analyze the influence of the parameter variation on the baseline.

This paper contains three parts. The first part is the introduction of the InSAR tethered satellites system. The second part describes the model of the system, baseline expression and numerical simulation of the InSAR tethered satellites system during the station keeping. The third part is the conclusion.

2. The Dynamic Model of The System

2.1. The TSS Model

The tethered satellites system is a complex system which could cause the attitude coupling. The system is disturbed by different kind of perturbations such as the solar radiation, the gravitation of the moon and the thermal effect of the tether. Compared to the tethered satellites, the InSAR tethered system has a shorter tether and is more flexible. Some assumptions are made to simplify the system.

1) The orbit of the mass center of system is Keplerian orbit.
2) The tether is a rigid rod.
3) The attitudes of the satellites keep relatively stable during the deployment.

The tethered satellites system could be seen in Fig. 1.

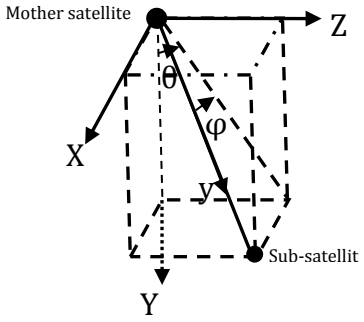

Figure 1. The tethered satellites system model

Newton-Eular law is used when deducing the dynamic equations. Three coordinates systems are used, the inertial coordinate $X_oY_oZ_o$, the orbit coordinate system XYZ fixed on the mass center and the line-of-sight frame xyz. The transfer matrix from xyz to XYZ is $\mathbf{C}$.

$$\mathbf{C}=\begin{bmatrix}\cos\varphi & -\sin\varphi & 0\\ \cos\theta\sin\varphi & \cos\theta\cos\varphi & -\sin\theta\\ \sin\theta\sin\varphi & \sin\theta\cos\varphi & \cos\theta\end{bmatrix} \tag{1}$$

θ and φ are the first and second rotational angle relatively, and the in-plane and out-plane vibration angles as well.

The angular velocity and the angular acceleration of the frame xyz are as following.

$$\boldsymbol{\omega}=\begin{bmatrix}\varpi+\dot{\theta}\\ 0\\ 0\end{bmatrix}+\mathbf{C}\begin{bmatrix}0\\ 0\\ \dot{\varphi}\end{bmatrix}=\begin{bmatrix}\varpi+\dot{\theta}\\ -\sin\theta\cdot\dot{\varphi}\\ \cos\theta\cdot\dot{\varphi}\end{bmatrix} \tag{2}$$

$$\dot{\boldsymbol{\omega}}=\begin{bmatrix}\ddot{\theta}\\ -\cos\theta\cdot\dot{\theta}\cdot\dot{\varphi}-\sin\theta\cdot\ddot{\varphi}\\ -\sin\theta\cdot\dot{\theta}\cdot\dot{\varphi}+\cos\theta\cdot\ddot{\varphi}\end{bmatrix} \tag{3}$$

ϖ is the mean orbital angular velocity of the mass center.

$$\varpi=\sqrt{\frac{u}{R_o^{\,3}}\left[1+\frac{J_2}{2}\left(\frac{R_\oplus}{R_o}\right)^2(3\sin^2\phi-1)\right]} \tag{4}$$

ϕ is the argument of latitude of the mass center. $R_\oplus$ is the mean radius of the earth and R_o is the instantaneous distance from the mass center to the geocenter.

$$\sin\phi = \sin i \sin(w + \vartheta) \tag{5}$$

i is the orbit inclination angle of the system. w is the argument of perigee. ϑ is the true anomaly of the system.

The position vector of the tether in the inertial frame is $\mathbf{r}$. The position vector of mother-satellite and sub-satellite are $\mathbf{R_m}$ and $\mathbf{R_s}$ relatively. The acceleration of the tether could be presented as following in inertial coordinate.

$$\ddot{\mathbf{r}} = \frac{\delta^2 \mathbf{r}}{\delta t^2} + 2\boldsymbol{\omega} \times \frac{\delta \mathbf{r}}{\delta t} + \boldsymbol{\omega} \times (\boldsymbol{\omega} \times \mathbf{r}) + \dot{\boldsymbol{\omega}} \times \mathbf{r} \tag{6}$$

$\frac{\delta^2 \mathbf{r}}{\delta t^2}$ and $\frac{\delta \mathbf{r}}{\delta t}$ are the acceleration and the velocity in the frame xyz.

Describe $\ddot{\mathbf{r}}$ in the xyz coordinate.

$$\ddot{\mathbf{r}} = \begin{bmatrix} -2\dot{\varphi}\dot{r}\cos\theta - r\ddot{\varphi}\cos\theta - r\varpi\dot{\varphi}\sin\theta \\ \ddot{r} - (\varpi + \dot{\theta})^2 r - r\dot{\varphi}^2 \cos^2\theta \\ 2(\varpi + \dot{\theta})\dot{r} + r\ddot{\theta} - r\dot{\varphi}^2 \sin\theta\cos\theta \end{bmatrix} \tag{7}$$

After getting the kinetic equations of the tether, the Newton-Eular law is used to get the dynamic equations. The force analysis could be seen in Fig. 2.

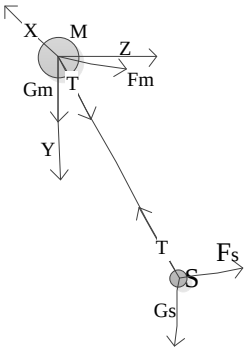

Figure 2. The force analysis of the system

The mother-satellite's dynamic vector description is as follow.

$$M_m \ddot{\mathbf{R}}_\mathbf{m} = \mathbf{G_m} + \mathbf{T} + \mathbf{F_m} \tag{8}$$

Then

$$\ddot{\mathbf{R}}_{\mathbf{m}} = -\frac{u}{R_o^{\,2}}[\mathbf{R_o} + \mathbf{R_{mo}} - \frac{3(\mathbf{R_o}\cdot\mathbf{R_{mo}})\mathbf{R_o}}{|\mathbf{R_o}|^2}]\left[1+\frac{J_2}{2}(\frac{R_\oplus}{R_m})^2(3\sin^2\phi-1)\right]+\frac{\mathbf{T}}{M_m}+\frac{\mathbf{F_m}}{M_m} \qquad (9)$$

In a similar way, the sub-satellite's dynamic equations could be also derived.

$$\ddot{\mathbf{R}}_{\mathbf{s}} = -\frac{u}{R_o^{\,2}}[\mathbf{R_o} + \mathbf{R_{so}} - \frac{3(\mathbf{R_o}\cdot\mathbf{R_{so}})\mathbf{R_o}}{|\mathbf{R_o}|^2}]\left[1+\frac{J_2}{2}(\frac{R_\oplus}{R_s})^2(3\sin^2\phi-1)\right]+\frac{\mathbf{T'}}{M_s}+\frac{\mathbf{F_s}}{M_s} \qquad (10)$$

In the above equations, $\mathbf{T}$, $\mathbf{F_m}$, $\mathbf{F_s}$ are the tether tension, the atmospheric drag of the mother-satellite and sub-satellite relatively.
The atmospheric drag of the sub-satellite could be described by $\mathbf{F_s}$.

$$\mathbf{F_s} = -\frac{1}{M_s}C_D A_s \frac{\rho_a}{2}\boldsymbol{\upsilon}_\mathbf{s}|\upsilon_s| \qquad (11)$$

υ_s is the velocity of the sub-satellite. In the orbit coordinate, υ_s is presented as follow.

$$\boldsymbol{\upsilon}_\mathbf{s} = \begin{bmatrix} l\dot{\varphi}+\dot{l}\sin\varphi \\ \dot{l}\cos\varphi\cos\theta \\ -\upsilon+\dot{\theta}l+\dot{l}\cos\varphi\sin\theta \end{bmatrix} \qquad (12)$$

υ is the orbital velocity of the mass center. l is the instantaneous length of the tether.

So the dynamic equation of the tether could be got.

$$\ddot{\mathbf{r}} = \ddot{\mathbf{R}}_\mathbf{s} - \ddot{\mathbf{R}}_\mathbf{M} = (-\varpi^2\mathbf{r} + \frac{3\varpi^2(\mathbf{R_o}\cdot\mathbf{r})\mathbf{R_o}}{|\mathbf{R_o}|^2}) + \frac{\mathbf{T}+\mathbf{F_s}}{M_s} - \frac{\mathbf{T}+\mathbf{F_m}}{M_m} \qquad (13)$$

Unfold the equation in the orbit frame.

$$
\begin{aligned}
\ddot{l} &= l(\varpi+\dot{\theta})^2\cos^2\varphi + 2l\varpi^2\cos^2\theta\cos^2\varphi + l\dot{\varphi}^2 - l\varpi^2\sin^2\varphi - l\varpi^2\sin^2\theta\cos^2\varphi \\
&\quad +2\dot{l}\dot{\varphi}\sin^2\theta\cos\varphi(\cos\varphi-\sin\varphi) - (\frac{1}{M_s}+\frac{1}{M_m})T + \frac{F_{my}}{M_m}\cos\varphi\cos\theta \\
&\quad -\frac{F_{sy}}{M_s}\cos\varphi\cos\theta - \frac{F_{mx}}{M_m}\sin\varphi + \frac{F_{sx}}{M_s}\sin\varphi + \frac{F_{mz}}{M_m}\cos\varphi\sin\theta - \frac{F_{sz}}{M_s}\cos\varphi\sin\theta \\
\ddot{\theta} &= -3\varpi^2\sin\theta\cos\theta - 2\frac{\dot{l}}{l}(\varpi+\dot{\theta}) + (\varpi+2\dot{\theta})\dot{\varphi}\tan\varphi - 2\frac{\dot{l}}{l}\dot{\varphi}\sin\theta\cos\theta\tan\varphi + \\
&\quad 2\frac{\dot{l}}{l}\dot{\varphi}\sin\theta\cos\theta + \frac{F_{mz}}{lM_m\cos\varphi}\cos\theta - \frac{F_{sz}}{lM_s\cos\varphi}\cos\theta - \frac{F_{my}}{lM_m\cos\varphi}\sin\theta \\
&\quad +\frac{F_{sy}}{lM_s\cos\varphi}\sin\theta \\
\ddot{\varphi} &= -\sin\varphi(\varpi+\dot{\theta})^2\cos\varphi - 2\varpi^2\cos^2\theta\cos\varphi\sin\varphi - \dot{\varphi}\tan\varphi - 2\frac{\dot{l}}{l}\dot{\varphi} - (\varpi^2-\dot{\varphi}^2)\tan\varphi \\
&\quad +\varpi^2\sin^2\varphi\tan\varphi + \varpi^2\sin^2\theta\cos\varphi\sin\varphi - 2\frac{\dot{l}}{l}\dot{\varphi}\sin^2\theta\sin\varphi(\cos\varphi-\sin\varphi) \\
&\quad -\frac{F_{my}}{lM_m}\cos\theta\sin\varphi + \frac{F_{sy}}{lM_s}\cos\theta\sin\varphi + \frac{F_{mx}}{lM_m}\sin\varphi\tan\varphi - \frac{F_{sx}}{lM_s}\sin\varphi\tan\varphi \\
&\quad -\frac{F_{mz}}{lM_m}\sin\varphi\sin\theta + \frac{F_{sz}}{lM_s}\sin\varphi\sin\theta + \frac{F_{sx}}{lM_s\cos\varphi} - \frac{F_{mx}}{lM_m\cos\varphi}
\end{aligned}
\tag{14}
$$

The above equations are the dynamic model of the system, from which it could be known that the system is highly nonlinear and coupling. Also, it is clear that the tether tension T is unknown. So it could be the control variable when deploying the system.

2.2. The expression of the baseline

Figure 3 shows the spatial geometric model of the InSAR tethered satellite system which is attributed to deduce the relationship between the baseline and the station parameters of TSS. The baseline vector $\mathbf{B}$ is from the antenna center mounted on the base-satellite to the antenna center fixed on the sub-satellite. B_x, B_y and $\mathrm{B_z}$ are the projected line-segment on the line-of-sight frame axis of the baseline vector. According to the Ref. [18], the spatial baseline of the system is restricted by B_y and B_z. The spatial baseline of system B_n could be expressed as follow:

$$
B_n = \left| B_z\cos\alpha + B_y\sin\alpha \right| \tag{15}
$$

In the Eq. 15, the variable α is the visual angle of antenna.

The baseline vector could vary if the TSS model changes, for example, the baseline vector of rod model is different from lump massed model. In the paper, lump massed

model is used when deducing the dynamic of TSS. Hence the baseline vector could be expressed as Eq. 16.

$$B = \sum_{i=1,\cdots,n} L_i \cos\theta_i \cos\varphi_i \tag{16}$$

In the Equation 16 n is the segment number of the tether. $L_i = L/n$, L is tether length.

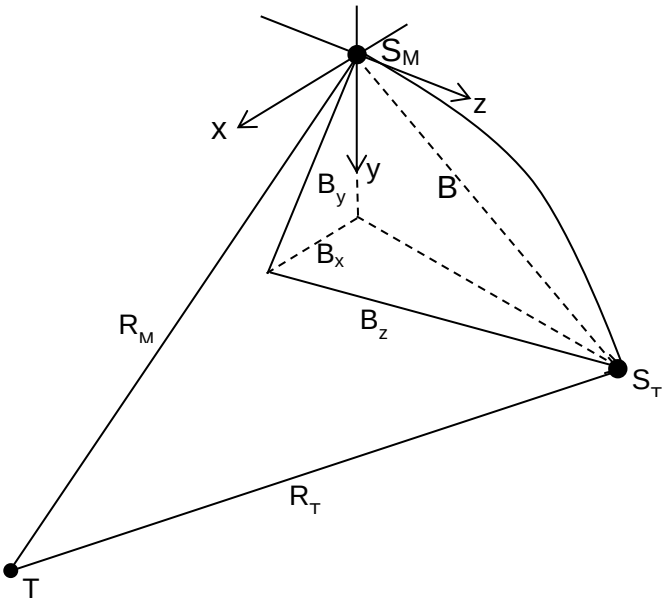

Figure 3. The baseline of the InSAR tethered satellite system

3. The Numerical Simulation

3.1. The numerical simulation of the tether flexibleness

The numerical simulations were conducted with different groups of initial parameter consisting of in-plane angle and out-plane angle to compare the effect caused by tether flexible with the motion affected by initial station. There are three groups initial parameter including different in-plane angles and out-plane angles. The in-plane angle and out-plane angle change from zero to 10°.

The system parameters used in simulation as follow: the base-satellite mass is $300kg$, sub-satellite mass is $100kg$, orbital altitude of TSS mass center is $200km$, the frontal area of base-satellite and sub-satellite are $2m^2$ and $1m^2$ respectively, the orbit inclination angle is 51.6° , the visual angle of antenna is 35.7° , the tether length $L = 2000m$ and the number of beads is 10.

The first group of initial parameters is $\theta = \varphi = 0$. Under the circumstance, the tether flexibility could be clearly seen with the Fig. 4 and Fig. 5. And the numerical results of this condition could be seen from Fig. 4 to Fig. 7.

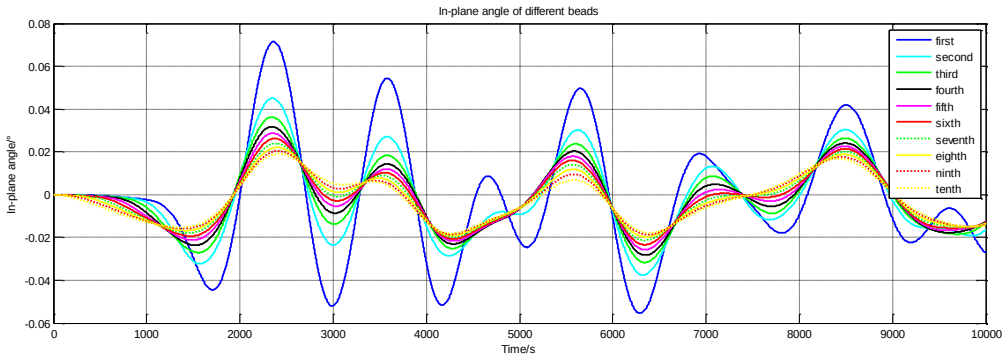

Figure 4. The In-plane angle variation of the different beads

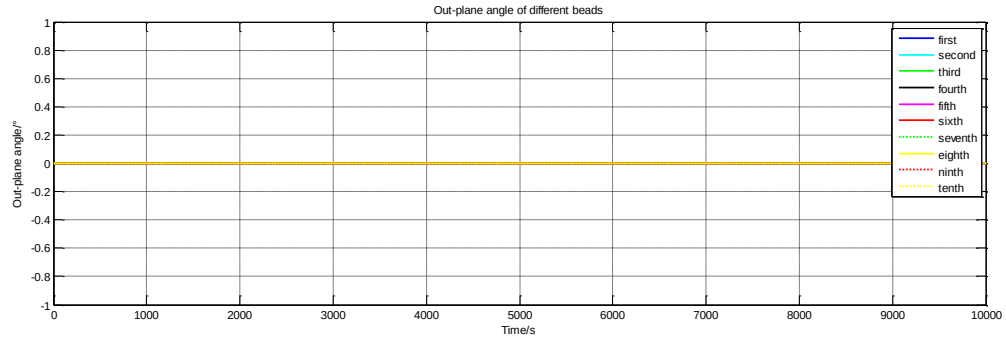

Figure 5. The Out-plane angle variations of the different beads

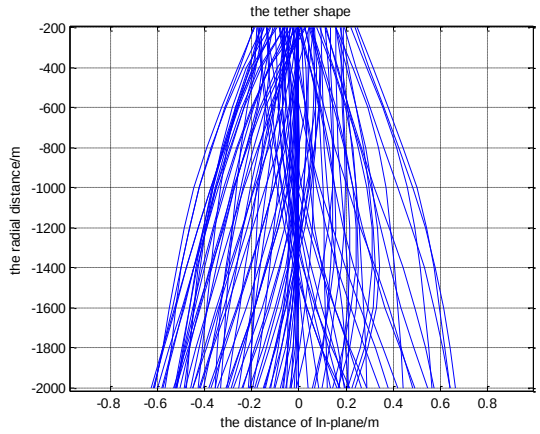

Figure 6. The tether shape variation

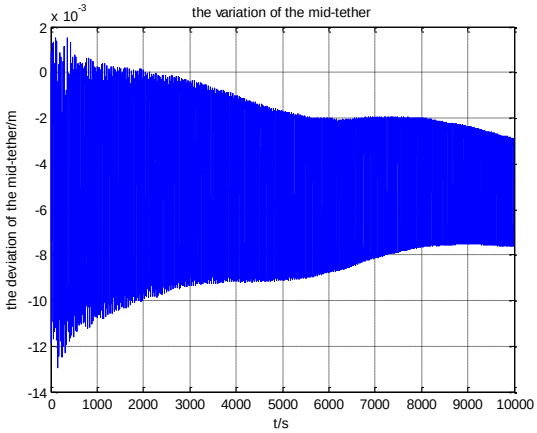

Figure 7. The deviation of mid-tether

These four pictures show the tether flexibility during the station keeping. Fig. 4 presents the in-plane angle of different beads. All the beads move similarly except the first bead. The frequency of the first bead is faster than others, which may be caused by the atmospheric drag, but not confirm. Basically, the amplitude of the beads is decreased along the increase of the distance from the bead to the base-satellite. And this is accordant with the Fig. 6. From the Fig. 6, the conclusion could be got that the tether is forward convex when the sub-satellite is before the base-satellite. Contrarily, the tether is backward convex when the sub-satellite moves behind the base-satellite in the orbital plane. Fig. 5 describes the out-plane angles of all beads keep zeroes. And Fig. 7 represents the deviation of mid-tether from the line connecting the

base-satellite and the sub-satellite. The amplitude of the deviation is very small, less than 0.013m.

The second group of initial parameters is $\theta = 10^{\circ}, \varphi = 0$. By changing the initial in-plane angle to investigate that if the initial angles have an effect on the bend degree of the tether. And the numerical results of this condition could be seen from Fig. 4 to Fig. 7.

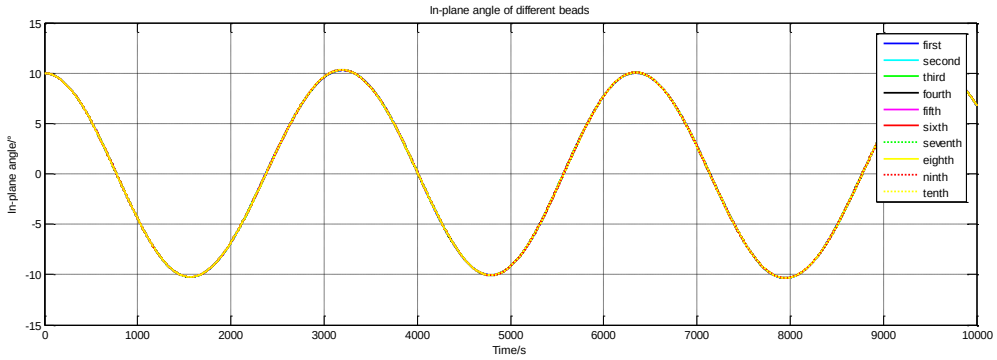

Figure 8a. the in-plane angle variation of different beads

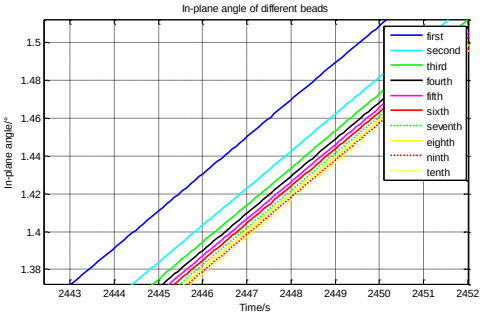

Figure 8b. The first augment of in-plane angle

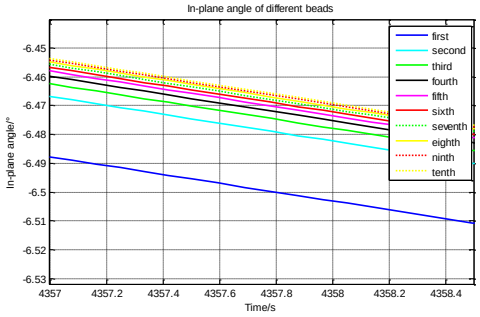

Figure 8c. The second augment of in-plane angle

The three pictures above shows the in-plane variation when initial in-plane angle isn't zero. The motion of beads is mainly affected by the initial condition. The in-plane angles of all beads change almost the same, but a little different which could be seen from the augment pictures Fig. 8b and Fig. 8c. Through the latter two graphs it could be known that the tether flexibility also has influence on the system's motion.

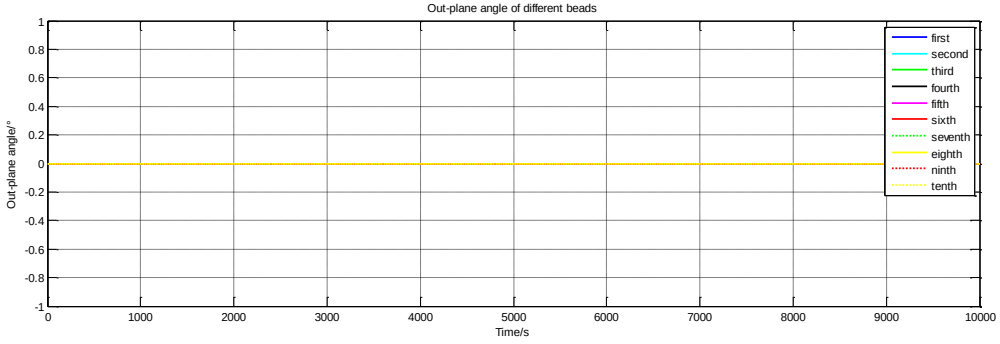

Figure 9. the out-plane angle variation of different beads

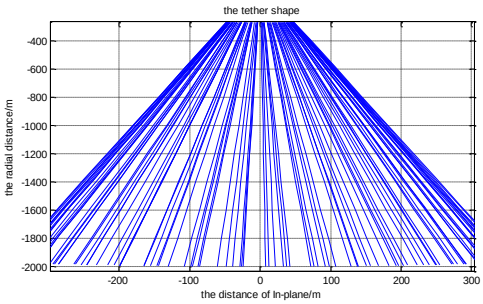

Figure 10. The tether shape variation

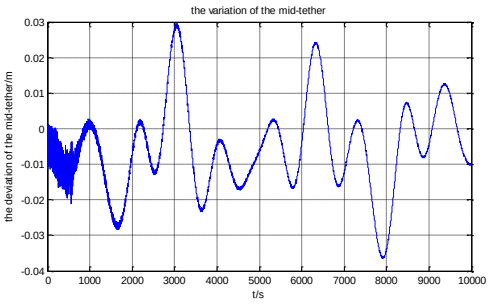

Figure 11. The deviation of mid-tether

Figure 9 shows the variation of out-plane angle keeping the same with the first circumstance. Fig. 10 proves the tether still bends like the first condition, forward when sub-satellite is before the base-satellite and backward when sub-satellite runs behind the base-satellite. Fig. 11 shows the deviation of the mid-tether is also small, but much bigger than the first circumstance.

After altering the in-plane angle from 0 to10°, the initial value of out-plane angle also is changed to10°. We know the in-plane motion is decided by the initial in-plane angle. Now the out-plane motion is simulated with the initial valuesθ=φ=10°. The numerical simulation result of this condition is from Fig. 12 to Fig. 15.

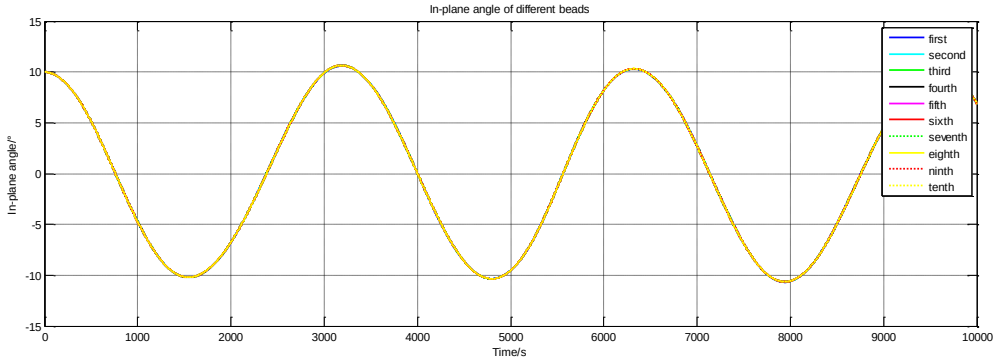

Figure 12a. the in-plane angle variation of different beads

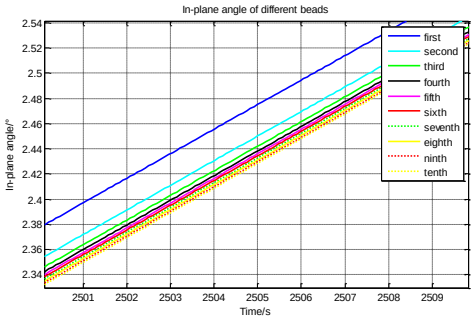

Figure 12b. the first augment of in-plane angle

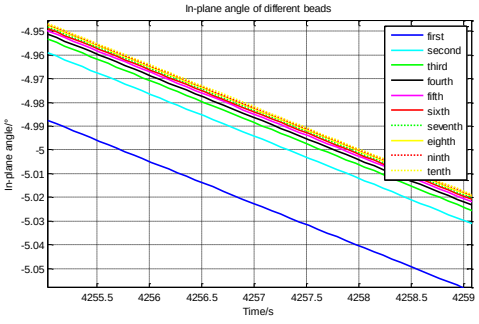

Figure 12c. the second augment of in-plane angle

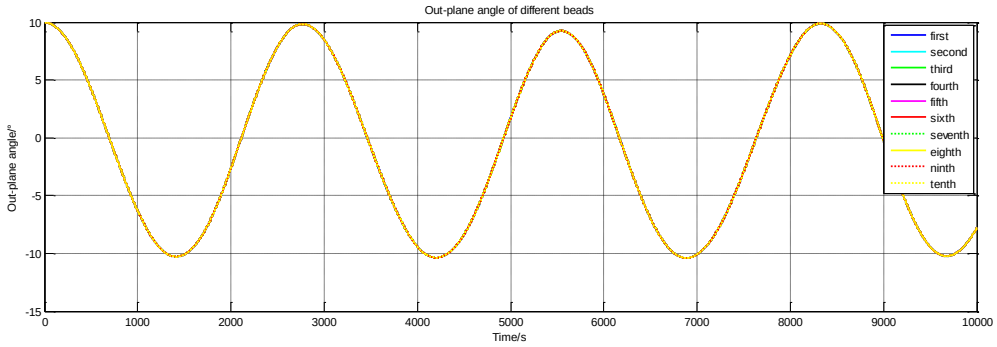

Figure 13a. the out-plane angle variation of different beads

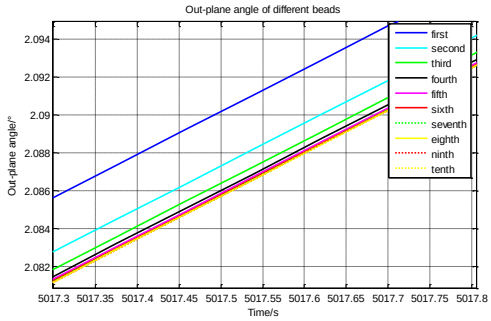

Figure 13b. the first augment of out-plane angle

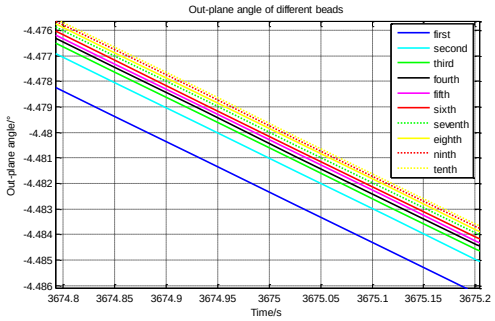

Figure 13c. the second augment of out-plane angle

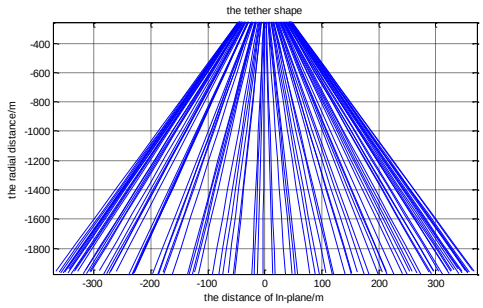

Figure 14. The tether shape variation

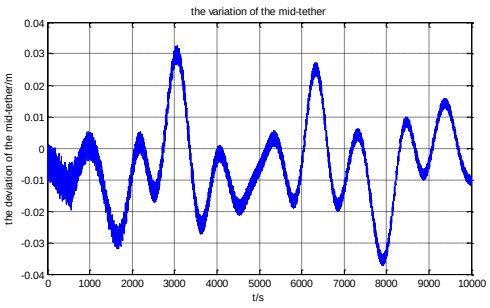

Figure 15. The deviation of mid-tether

The in-plane angle variation is very similar with the out-plane angle variation excluding that the vibration frequency of out-plane is larger than that of in-plane. And the angle variations of all beads are different because of the tether flexibility; however, it is negligible compared to the vibration caused by initial angles according to the Fig. 12 and Fig. 13.

The tether still bends like before mentioned in the orbital plane. But in perpendicular plane the tether curves forward when the out-plane angle is larger than zero, which is similar with the in-plane motion. Fig. 15 shows that the deviation of mid-tether is mainly affected by in-plane angle.

The numerical simulation shows that the system motions is mainly affected by the initial angles of in-plane and out-plane. The tether is not a line for the tether flexibility,

but the effect on the motion caused by tether flexibility is insignificant compared to the motion caused by initial angles.

3.2. The Baseline Variation Simulation

The baseline could be expressed as Eq. 16. Then the simulation of baseline variation was conducted to figure out the effect of system station and tether flexibility on the baseline variation. The parameters used are the same with before. The numerical results are from the Fig. 16 to Fig.20.

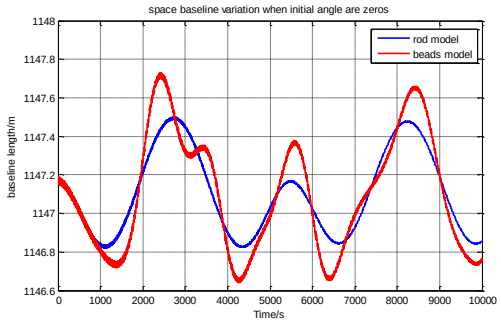

Figure 16. the baseline variation with zero initial angles

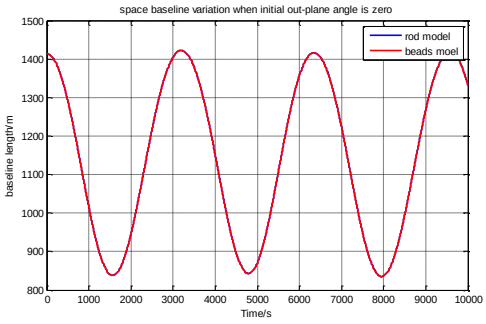

Figure 17. the baseline variation when in-plane angle is not zero

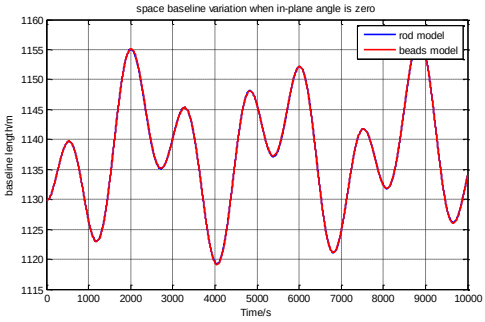

Figure 18. the baseline variation when out-plane angle is not zero

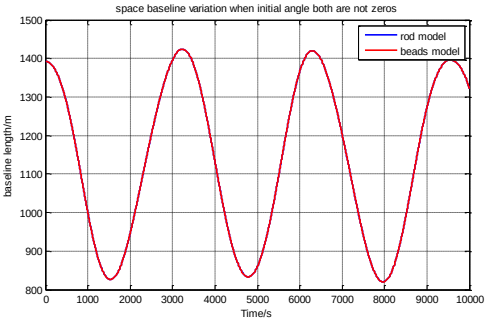

Figure 19. the baseline variation when angles both not zero

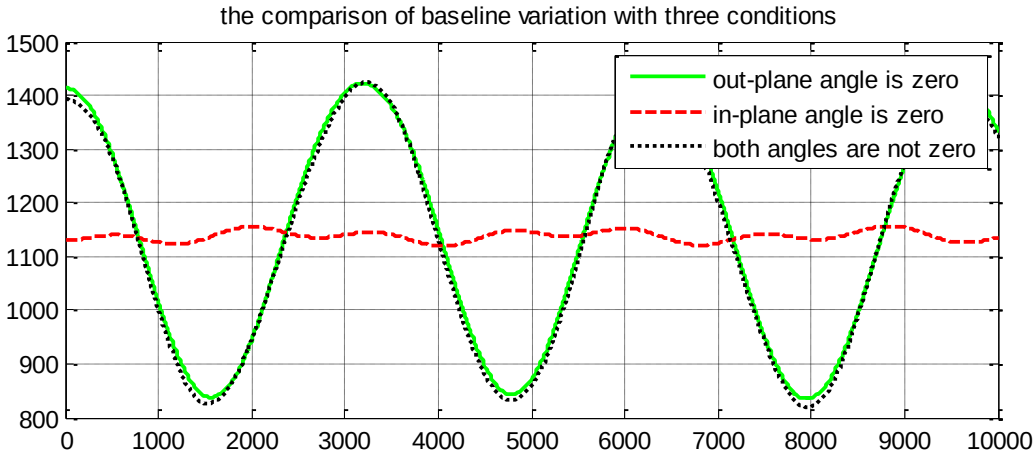

Figure 20. the comparison of three conditions

The first four pictures describe the baseline variation using different models with three conditions. The blue presents the rod model and red represents the beads model which could take account of the tether flexibility. These four pictures prove that comparing to system station the tether flexibility has little effect on the baseline variation during the station keeping. However, the baseline variation when the in-plane and out-plane are both not zero is more similar with the condition of zero out-plane angle. From Fig. 16, it could be seen that the tether flexibility still has effect on the baseline variation. The variation frequencies of two models are close and the amplitude of bead model is higher because of the tether flexibility. But when there is vibration of the system, the baseline variation is mainly affected by the vibration caused by initial angles.

It is clearly that baseline variation between Fig. 17 and Fig. 18 is different. But the Fig. 19 looks like Fig. 17. To further investigate the condition, these three circumstances are compared in Fig. 20 using the beads model. When in-plane angle is zero, the baseline varies in a narrow scope, which is insignificant when the in-plane angle equals the out-plane angle. Therefore, the variation when both angles are not zero is different with another curve indicating the variation when out-plane is zero. So the baseline variation is related to all these factors, but mainly the in-plane vibration.

4. Conclusion

After deriving the dynamics of the InSAR tethered satellite system, some findings about the system's motion and baseline variation were made through the numerical simulation. The in-plan vibration and the out-plan vibration are the quasi-periodic motion and the amplitudes mainly determined by the initial parameters. The tether's shape is a curve whose curvature changes along with time, but the magnitude is pretty small. And the system motions are mainly affected by the initial angles of in-plane and out-plane. Moreover, the effect on the motion caused by tether flexibility is insignificant compared to the motion caused by initial angles. The tether flexibility has little effect on the baseline variation; however it is mainly determined by the in-plane vibration.

But the model used in the paper differs from the real system; a flexible model may get more accurate results compared to the lumped mass model. In this paper, only relationship between the baseline and the system parameters was investigated. But how to adjust the baseline and design of the InSAR tethered satellite system need to further research.

5. Acknowledgements

The authors are sincerely grateful to the Research Center of Satellite Technology for offering the favorable environment. The authors also thank all the researchers in the institute who made fruitful comment.

6. References

[1] Colombo, G., Gaposchkin, E.M., Grossi, M.D., et al, “The Skyhook: A shuttle borne tool for low-orbital-altitude research,” Meccanica, Vol. 10, 1975, pp. 3-20.

[2] Kumar, K.D., “Review of dynamics and control of nonelectrodynamic tethered satellite systems,” Journal of Spacecraft and Rockets, Vol. 43, 2006, pp. 705-720.

[3] Micheal, V. P., “Space Tethers and Space Elevators,” 2009, pp. 59-92.

[4] Cartmell, M. P., McKenzie, D. J., “A review of space tether research,” Progress in Aerospace Sciences, Vol. 44, 2008, pp. 1-21.

[5] Cheng, Y. M., Cho, S., Cochran, J. E., “Orbital dynamics of tethered satellite systems,” Astrodynamics 1997, 1998, pp.61-69.

[6] Krupa, M., Poth, W., Schagerl, M., et al, “Modelling, dynamics and control of tethered satellite systems,” Nonlinear Dynamics, Vol. 43, 2006, pp. 73-96.

[7] Misra, A. K., “Dynamics and control of tethered satellite systems,” Acta Astronautica, Vol. 63, 2008, pp. 1169-1177.

[8] Bainum, P. M., Kumar, V. K., “Optimal control of the Shuttle-Tethered-Subsatellite system,” Acta Astronautica, 1980, Vol. 7, pp. 1333-1348.

[9] Slane, J. H., Tragesser, S., “Stability of tethered satellites using Folquet theory for a non-equilibrium reference,” Advances in the Astronautical Sciences, 2008, Vol. 130, pp. 729-738.

[10] Liaw, D. C., Abed, E. H., “Stabilization of tethered satellites during station keeping,” IEEE Transactions on Automatic Control, 1990, Vol. 35, pp. 1186-1196.

[11] Vetrella, S., Moccia, A., “The tethered satellite system as a new remote-sensing platform,” International Journal of Remote Sensing, 1987, Vol. 8, pp. 369-383.

[12] Light, D. L., “Characteristics of Remote Sensors for Mapping and Earth-Science Applications,” Photogrammetric Engineering and Remote Sensing, 1990, Vol. 56, pp. 1613-1623.

[13] Krieger, G., Moreira, A., Fiedler, H., et al, “TanDEM-X: A satellite formation for high-resolution SAR interferometry,” IEEE Transaction on Geoscience and Remote Sensing, Vol. 45, pp. 3317-3341.

[14] Moccia, A., “A tethered interferometric synthetic aperture radar (SAR) for a topographic mission,” IEEE Transaction on Geoscience and Remote Sensing, 1992, Vol. 30, pp. 103-109.

[15]Quadrelli, M., “Modeling and dynamics of tethered formations for space interferometry,” 11th AAS/AIAA Space Flight Mechanics Meeting, 2000, pp. 1-3.

[16] Vogel, K. A., “Dynamics and control of tethered satellite formations for the purpose of space-based remote sensing,” Air Force Institute of Technology, 2006, pp. 1-4.

[17] Grassi, M., Moccia, A., Vetrella, S., “attitude control by inertia wheels of a tethered interferometric SAR for topographic mapping,” Meccanica, 1993, Vol. 28, pp. 333-339.

[18] Chen, J., Zhou, Y. Q., Li, C. S., “Baseline design and performance analysis for distributed spaceborne interferometric synthetic aperture radar,” Acta Electronica Sinica, 2004, Vol. 32, pp. 1974-1977.